Transverse Relaxation Time Reflects Brain Amyloidosis in Young APP/PS1 Transgenic Mice

Nadine El Tannir El Tayara,[1,2] Andreas Volk,[1,2] Marc Dhenain,[1–3]* and Benoît Delatour[4]

Amyloid deposits are one of the hallmarks of Alzheimer's disease (AD), one of the most devastating neurodegenerative disorders. In transgenic mice modeling Alzheimer's pathology, the MR transverse relaxation time (T_2) has been described to be modulated by amyloidosis. This modification has been attributed to the age-related iron deposition that occurs within the amyloid plaques of old animals. In the present study, young APP/PS1 transgenic mice without histochemically detectable iron in the brain were specifically studied. In vivo measurements of T_2 in the hippocampus, at the level of the subiculum, were shown to reflect the density of amyloid plaques. This suggests that T_2 variations can be induced solely by aggregated amyloid deposits in the absence of associated histologically-detectable iron. Thus T_2 from regions with high amyloid load, such as the subiculum, is particularly well suited for following plaque deposition in young animals, i.e., at the earliest stages of the pathological process. Magn Reson Med 58:179–184, 2007.

Key words: Alzheimer's disease; amyloid-β peptide; iron; T_2; transgenic mouse

Alzheimer's disease (AD) is characterized by two main neuropathological lesions: senile plaques and neurofibrillary tangles. Plaques are extracellular deposits of amyloid-β (Aβ) peptides, while tangles are intraneuronal filaments of hyperphosphorylated tau proteins (1). Until now, the definitive diagnosis of AD has required postmortem detection of these lesions. According to the amyloid cascade hypothesis, abnormal amyloid accumulation in the brain is a critical event in the disease process (2). Therefore, the development of disease modifiers targeting Aβ pathology appears to be of crucial importance.

Imaging strategies aimed at in vivo detection of cerebral Aβ deposition in mice are being actively investigated to monitor the progression of disease and assess the effects of new therapies. Until now, most of the protocols that allowed detection of brain amyloidosis in a noninvasive way in animals have relied on magnetic resonance imaging (MRI). Two strategies were developed. The first one is based on the direct detection of individual amyloid plaques by MR microimaging. This approach either exploits the natural contrast of the plaques (3) or uses specific contrast agents targeting Aβ (4–6). This approach is hampered by the difficulty of imaging the smallest plaques because of the limited resolution of the MRI. The second strategy looks for "global" relaxation time changes associated with the presence of Aβ instead of trying to detect individual plaques. For instance, it has been demonstrated that the transverse relaxation times (T_2) of brain tissues from aged mouse models of AD are modified by the presence of Aβ deposits associated with iron (7–9). The aim of the present study was to better understand and refine the origin of T_2 modifications observed in plaque-enriched brain tissue from living mice modeling AD cerebral amyloidosis. These modifications may be caused by different/concurrent factors, such as the presence of hydrophobic amyloid deposits or age-related accumulation of iron within the plaques (3,9,10). To assess the impact of each factor, the present study focused on young to middle-aged APP/PS1 transgenics (16–31 weeks of age).

In several animal species, including humans, cerebral iron increases with age and reaches a plateau in mature adults (11). In mice, an age-related increase of iron load seems to occur between the age of 2.8–3.4 months and 11 months (12,13). In a previous study we suggested that iron originating from surrounding tissue becomes progressively associated with plaques in old double APP/PS1 transgenic mice (9). Interestingly, in this transgenic line, brain amyloidosis is very aggressive, with an early onset at 2.5 months (14), presumably a few weeks before the increase of cerebral iron load occurs. Thus, one can expect young APP/PS1 mice to start developing plaques without presenting an amyloid-associated iron load, which gives investigators an opportunity to isolate and refine the role of amyloid-β deposition per se on MR relaxation times. Indeed, in the present work, the youngest mice studied did not show histologically detectable iron deposition while still presenting variable amyloid loads. Analysis of regional T_2 relaxation times was performed in the subiculum, one of the first brain areas to develop Aβ plaques in the studied transgenic model (14), and in the temporal association cortex, in which no amyloid deposits were detected even in the oldest animals studied. We showed that even before the occurrence of histologically detectable iron in the plaques, the subicular T_2 is negatively correlated to the amyloid load. This suggests that amyloid deposits or tissue modifications associated to amyloid deposits have a direct effect on T_2, and that this parameter can be used as an early, iron- and age-independent biomarker of the amyloid load.

MATERIALS AND METHODS

Transgenic Mice

Transgenic APP/PS1 mice (Thy1 APP751 SL (Swedish mutation KM670/671NL, London mutation V717I introduced in

[1]INSERM, U759, Centre Universitaire, Orsay, France.
[2]Institut Curie Research Center, Centre Universitaire, Orsay, France.
[3]CEA, SHFJ, URA CEA CNRS 2210, Orsay, France.
[4]Laboratoire NAMC, CNRS, UMR 8620, Bât 446, Université Paris Sud, Orsay, France.

Grant sponsors: Aging ATC 2002 (INSERM); Fédération pour la Recherche sur le Cerveau 2003; Del Duca Foundation; ACI Neurosciences 2004 (French Research Department).

*Correspondence to: Marc Dhenain, URA CEA CNRS 2210, SHFJ, 4 Place du Général Leclerc, 91401 Orsay Cedex, France. E-mail: Marc.Dhenain@cea.fr

Received 17 August 2006; revised 8 March 2007; accepted 15 March 2007.
DOI 10.1002/mrm.21266
Published online in Wiley InterScience (www.interscience.wiley.com).

human sequence APP751) × HMG PS1 M146L), modeling early onset (at 9–14 weeks of age) and progressive cerebral amyloid deposition ($N = 11$, 16–31 weeks of age) were used (14). Heterozygous "APP/PS1" mice were obtained by crossing heterozygous Tg $APP_{(+/-)}$ mice with homozygous Tg $PS1_{(+/+)}$ mice. The $APP_{(-/-)}/PS1_{(+/-)}$ mouse littermates ("PS1") resulting from crossings were used as controls ($N = 10$, 16–31 weeks of age) because they display no amyloid plaques and therefore allow one to specifically evaluate the effects of the APP transgene on amyloid deposition in the brain.

In Vivo MRI Experiments and Data Analysis

In vivo MR images were recorded on a 4.7-Tesla Bruker Biospec 47/30 system equipped with a 12-cm-diameter gradient system (200 mT/m). A surface coil (diameter = 30 mm), actively decoupled from the transmitting birdcage probe (Bruker GmbH), was used for signal acquisition. The animals were anesthetized with isoflurane (5% for induction, 1–1.5% for maintenance) in a mixture of N_2 (80%) and O_2 (20%) administered via a face mask. The respiration rate was monitored to ensure the animals' stability until the end of the experiment. The body temperature of the mice was maintained by using a water-filled heating blanket.

The MRI protocol was previously described (9). Briefly, a multislice multiecho sequence was used for T_2 measurements (echo times (TEs) = 12.2, 24.4, 36.6, 48.8, 61, and 73.2 ms; repetition time (TR) = 2000 ms; field of view (FOV) = 1.5 × 1.5 cm^2; matrix = 128 × 128; slice thickness = 1 mm; acquisition time = 8 min 49 s). Parametric T_2 maps were generated by fitting pixel intensity values to single exponential curves using the Bruker fit package.

Inversion-recovery images (TE = 10 ms, TR = 5000 ms, TI = 300 ms, FOV = 1.5 × 1.5 cm^2, matrix = 128 × 128, slice thickness = 1 mm) that had good contrast between cerebral structures were acquired to localize regions of interest (ROIs) corresponding to the subiculum and the temporal association cortex. The subiculum is one of the first regions to show plaque deposition in APP/PS1 mice, while the temporal cortex undergoes amyloidosis much later during the disease process. The ROI corresponding to the subiculum was placed underneath the cingulum on a slice localized approximately between bregma –2.8 mm and bregma –3.8 mm according to the Paxinos atlas (15). ROIs corresponding to the temporal association cortex were drawn on this same slice. ROI outlines were then transferred to T_2 maps. For all animals the T_2 values were the mean of ROIs drawn on the left and right sides of the brain, except for one APP/PS1 animal and one PS1 animal in which T_2 values were issued from only one side of the brain where the cingulum was accurately localized.

Histological Analysis

Following completion of the MRI studies, the mice were killed by decapitation. Their brains were then extracted and fixed in 10% buffered formalin and kept in fixative at −4°C until they were processed for histology (mean fixation time ± SEM: 51 days ± 7 days). The brains were then stored overnight in a solution of 20% glycerin and 2% dimethylsulfoxide in 0.1-M phosphate buffer for cryoprotection. They were subsequently sectioned into 10 series of 40-μm-thick coronal sections on a freezing microtome.

Anti-Aβ immunohistochemistry was performed using the biotinylated 4G8 antibody (Biovalley, France). Endogenous peroxidase activity and nonspecific antigenic sites were first blocked using standard procedures before incubation with primary antibodies (1/10000, one night at room temperature). Following incubation in avidin-biotin-horseradish peroxidase complex (Vector Laboratories, Burlingame, CA, USA), the final reaction made use of 3-3′-diaminobenzidine as the chromogen (brown product). Amyloid deposits were concurrently labeled by standard Congo red staining on a second batch of slices (adapted from Ref. 16). Each Congo-red-stained slice was digitized using a Super CoolScan 8000 ED high-resolution scanner (Nikon, Champigny sur Marne, France). Regional amyloid loads (expressed as the percentage of tissue surface stained by the Congo red dye) were quantified in the subiculum area that was previously investigated by means of MRI, using computer-based thresholding methods (17). Each stained section was binarized after thresholding in Photoshop (Adobe Systems, Paris, France). The binarized images were then transferred to Image-Pro Plus software (Media Cybernetics, Silver Spring, USA) and submitted to a particle-detection algorithm to measure the surface of plaques on each brain section (two to four sections sampled per mice). The proportion of tissue area occupied by Congo-red-stained material was then assessed. The ratio (surface stained/whole subiculum ROI surface) was taken as a measure of the "amyloid load" in the subiculum.

Iron staining was performed on a third batch of serial sections using a protocol derived from the standard Perls-diaminobenzidine (Perls-DAB) method as previously described (9,18). Although biochemical quantification of iron (e.g., atomic absorption spectrophotometry) is the most valuable and precise method to assess iron concentrations, this approach was discarded as it can not be used to measure iron loads in discrete brain areas. Quantification of Perls-stained material has been proven to reflect iron concentrations (19,20) as a linear relationship exists between the two measurements (20). In our experiments, final intensification with diaminobenzidine of the Perls stain was carefully monitored under the microscope to obtain the best signal-to-noise ratio (SNR) with a compromise between clear labeling and rising background staining. Brain slices for all mice were simultaneously processed, and incubation in DAB was performed for the same duration in all animals.

RESULTS

Neuropathological examination showed amyloid plaques in the subiculum of all studied APP/PS1 mice (Fig. 1). On the contrary, no plaques were observed in the temporal cortex, even in the oldest animals (Fig. 1c). Noticeably, intracytoplasmic positive 4G8 staining was found in the neurons of the subiculum, but not in other brain areas, of the three youngest mice (Fig. 1j). In older mice, cytoplasmic immunostaining of subicular neurons was lacking or only very faint. As expected, PS1 mouse brains were plaque-free. Quantitative analysis showed that in the subiculum of APP/PS1 mice the Congo red-assessed amyloid

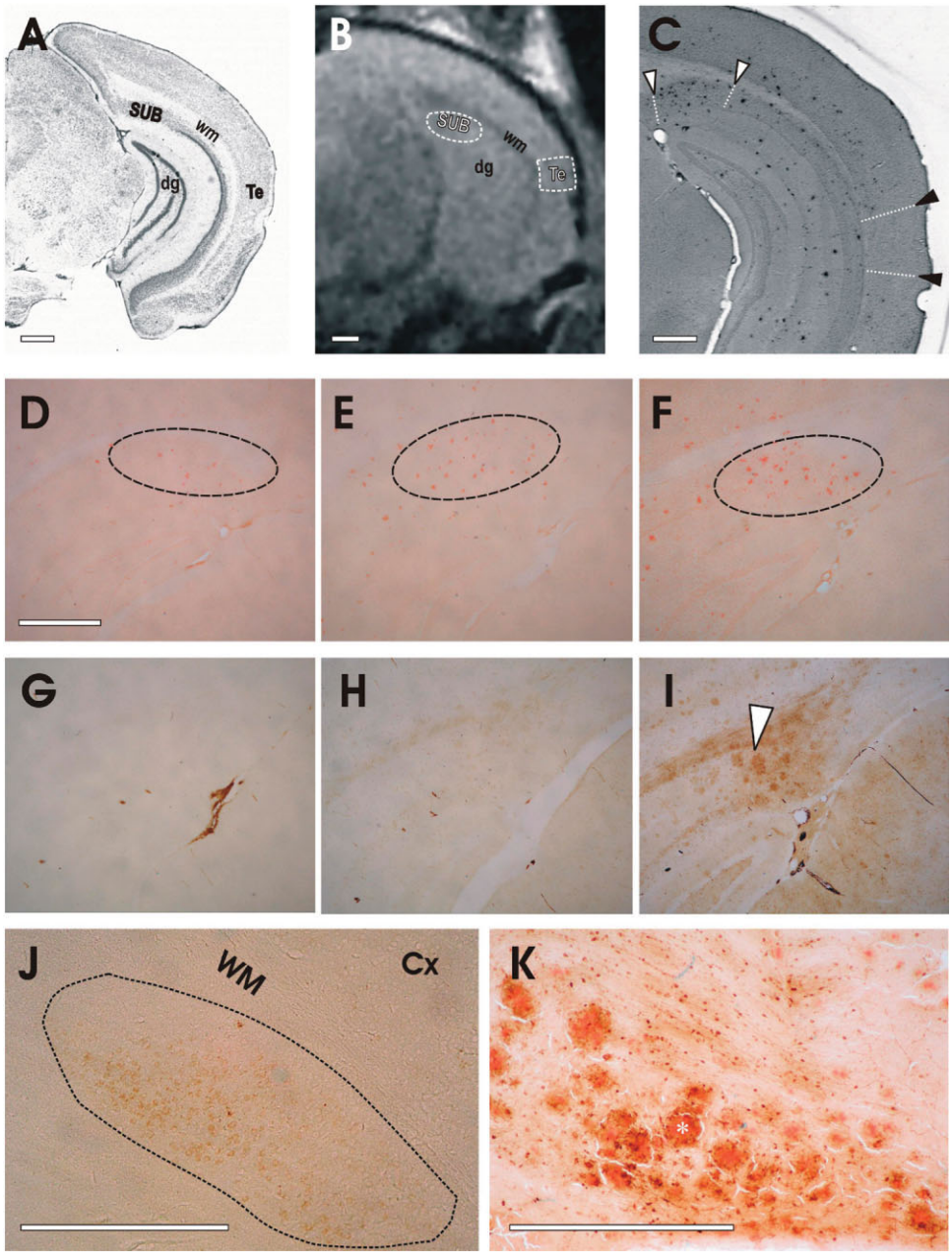

FIG. 1. Neuropathology of APP/PS1 mice. **a:** Brain slice (Nissl stain) illustrating the anatomical level where the subicular (SUB) and temporal cortical (Te) regions were sampled for both MRI and histological measurements (dg: dentate gyrus of the hippocampus; wm: white matter). **b:** MR image (inversion-recovery protocol (TR/TE/TI = 5000/10/300 ms)) illustrating the regions where T_2 values were evaluated (labels as in **a**). **c:** Amyloid deposition in an old APP/PS1 mouse (31 weeks old) showing Congo-red-stained plaques in the hippocampus, including the subiculum (white arrowheads) but a paucity of brain amyloidosis in the cortical mantle, especially at the level of temporal regions (black arrowheads). **d–f:** Congo red stain to visualize amyloid deposits in the subiculum (area delimited by dotted lines) of APP/PS1 mice at different ages (**d:** 16 weeks; **e:** 22 weeks; **f:** 27 weeks). Note the gradual increase of plaque density with progressive aging. **g–i:** Perls stain to detect iron in the brain of the same mice as shown in **d–f**. Iron is virtually absent in the two youngest animals (**g** and **h**), but is clearly detectable in the 27-week-old mouse (**i**), where it colocalized with amyloid plaques (white arrowhead). **j:** Intraneuronal accumulation of Aβ (4G8 immunostaining) in neurons of the subiculum (outlined area) of a 16-week-old APPxPS1 mouse. Note that only cells from the subiculum contain cytoplasmic Aβ. Cx: overlying cortex. **k:** Double Congo red + Perls-DAB stain in a 30-week-old APP/PS1 mouse showing the association of amyloid plaques (red) and iron (brown). The asterisk indicates one example of amyloid plaque engulfed in iron deposits. All scale bars: 500 μm (same scale bar for **d–i**).

load was correlated with the age of the animals ($r = 0.64$, $P < 0.05$). In this region, iron was associated with the amyloid plaques of mice older than 23 weeks (Fig. 1k) but was not histologically detected in younger animals (compare Fig. 1g and h with Fig. 1i).

MRI measurements performed on living mice before the neuropathological examination indicated significantly lower T_2 values in the subiculum of APP/PS1 mice as compared to age-matched PS1 animals ($U = 22.5$, $P < 0.02$; nAPP/PS1 = 11, nPS1 = 10; Fig. 2). On the contrary, no

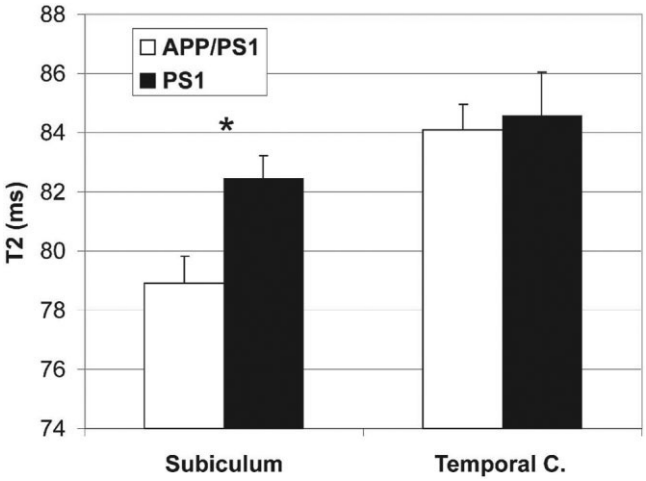

FIG. 2. T_2 values in APP/PS1 and control PS1 mice. In the plaque-enriched subicular region, T_2 was significantly reduced in double APP/PS1 transgenics ($N = 11$; mean age: 21.9 ± 1.4 weeks) as compared to plaque-free PS1 mice ($N = 10$; mean age: 21.7 ± 1.9 weeks). On the contrary, no genotype effect was noted when T_2 was measured in the temporal cortex. Importantly, this isocortical brain region was amyloid-free in the studied APP/PS1 mice due to their young age (range: 16–31 weeks). *$P < 0.02$.

differences between T_2 values in the temporal cortex of APP/PS1 and PS1 mice (Mann-Whitney U = 51, ns; Fig. 2) were noticed.

Correlative analysis revealed a significant negative linear relationship between T_2 values and amyloid load in the subiculum of APP/PS1 mice ($r = -0.77$, $P < 0.01$). This negative correlation was preserved even when analysis was restricted to the youngest APP/PS1 animals, in which amyloid was not associated with histochemically detected iron (age = <23 weeks; $N = 8$, $r = -0.8$, $P < 0.05$; Fig. 3). Importantly, for PS1 and APP/PS1 animals of the same age group, T_2 values were not significantly correlated with age regardless of the brain region evaluated.

A population analysis of the youngest mice (age = <23 weeks) with no histologically-detected iron in the subiculum revealed that the subicular T_2s of PS1 mice ($N = 7$) were in the same range as those of APP/PS1 mice with lower amyloid loads (<7%; U = 13, ns), but were statistically longer than those of APP/PS1 mice with higher amyloid loads (>7%, U = 0, $P < 0.02$). Finally, in agreement with correlative data (see above), the T_2s of APP/PS1 mice with no histologically-detected iron but presenting a high amyloid load was significantly shorter than those of iron-free APP/PS1 mice with a low amyloid load (U = 0, $P < 0.05$).

DISCUSSION

T_2 is Reduced in the Subiculum of APP/PS1 Mice

T_2 values were assessed in the subiculum and temporal cortex of double transgenic APP/PS1 mice modeling early-onset and progressive amyloid deposition, and in single transgenic PS1 animals that were used as amyloid deposit-free controls. The use of PS1 littermates as controls allowed us to specifically assess the effects of amyloid deposition on T_2. We first showed that T_2 values measured in vivo were lower in the subiculum of APP/PS1 than in PS1 mice. This result, obtained in a cohort of young adults (16–31 weeks), confirms previous data obtained in older animals (27–45 weeks of age) (9).

In the present study, the lack of T_2 changes in the temporal cortex of APP/PS1 mice as compared to PS1 animals might be explained by a lack of cortical plaques in this brain region in the APP/PS1 mice. However, in a previous work (9) we also showed that T_2 was not modified in the cortex of older APP/PS1 animals that displayed plaques in the isocortex. For those aged animals, the lack of T_2 differences between genotypes may be related to the relatively low amyloid load in the isocortex (as compared to the subiculum), but more likely is related to the high and equal amounts of cortical iron deposition (associated or not with the amyloid plaques) in old APP/PS1 and PS1 mice, which may mask the T_2 effect caused by amyloid plaques per se.

Amyloid Deposits Lead to a T_2 Decrease Even in the Absence of Detectable Iron

It is well known that iron accumulates in amyloid plaques (21,22). Thus, several studies have suggested that the T_2 decrease in the brain of transgenics with brain amyloidosis may be associated with the effect of iron on relaxation

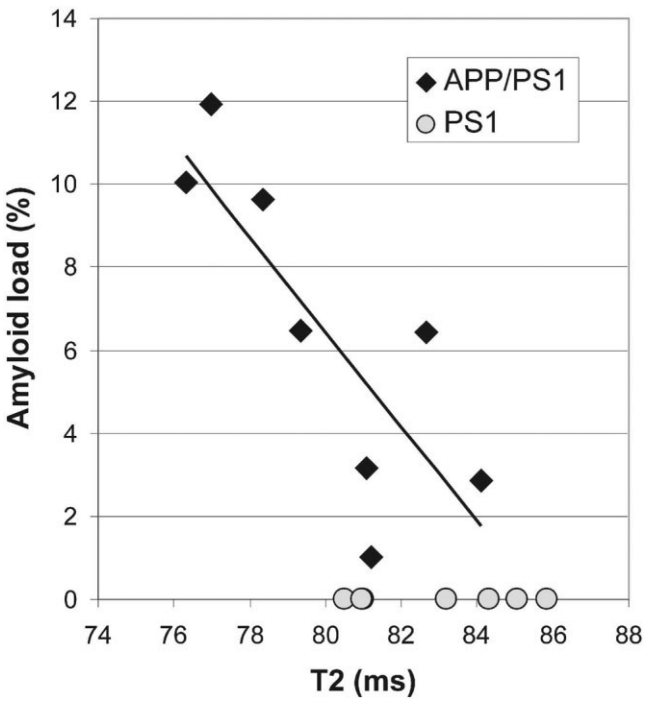

FIG. 3. Association between in vivo T_2 and amyloid load in the subiculum. The correlation between amyloid load and subicular T_2 value was studied in the youngest APP/PS1 mice (age = <23 weeks; $N = 8$) in which iron was not histochemically detected in plaques and therefore did not compete with amyloid-related effects on MR relaxation times. A negative correlation was observed between in vivo MRI measurements and plaque load ($r = -0.8$, $P < 0.05$). Note that the PS1 mice display subicular T_2 values that are in the same range as those of APP/PS1 mice with the lowest (<7%) amyloid load.

times (7,10). In a previous study we showed nevertheless that the overall brain iron load is not modified in APP/PS1 mice as compared to PS1 mice, and only its local distribution is altered between genotypes (i.e., while iron is focally distributed in amyloid plaques in APP/PS1 mice, it is diffusely deposited in control PS1 animals). Iron presence within the plaques can explain the ability to detect the plaques by MR microimaging. Regarding the global T_2 decrease reported in previous studies, one might suspect that iron distribution in focal aggregates leads to a T_2 decrease via a "magnetic relaxation switch" effect (9,23). However, another possible explanation is that the T_2 decrease observed in APP/PS1 mice is related to the density of plaques per se. The present study, which showed a negative correlation between T_2 values and amyloid load in a cohort of young mice that displayed subicular amyloid plaques without detectable iron aggregates, indeed strongly supports this hypothesis. Our results indicate that mechanisms other than those associated with focal iron deposition within the plaques may be responsible for the reduced T_2 relaxation in tissue containing amyloid deposits. Several mechanisms may account for this effect. First, the hydrophobic nature of amyloid deposits may be responsible for T_2 shortening. However, some other tissular alterations associated with the accumulation of amyloid plaques may be involved. For instance, we detected intraneuronal amyloid β proteins in the subiculum of the youngest APP/PS1 mice studied. This feature was previously described in the same mouse model used in the present study (24). The presence of amyloid-β peptides in the intracellular space modifies cell physiology and is considered to be a critical event and primary physiopathological step in AD (see Ref. 25 for a review). Thus the T_2 relaxation time, which can be a sensitive indicator of impaired cell physiology (26), can be affected. The observed T_2 reduction may also result from other pathological processes (e.g., hypoperfusion (27)) associated with the amyloid load. It has been shown that mouse models of AD have decreased cerebral blood flow and/or blood volumes, which are associated with Aβ pathology (28), and that T_2 is sensitive to a reduction in the cerebral blood flow (27). Further studies are needed to determine the relevant relaxation processes and the extent to which these factors affect the T_2 relaxation time.

T_2 Is an Early In Vivo Marker of Amyloid Deposition

Previous methods to directly detect plaques by MR microimaging require a difference in T_2 between plaques and brain tissue, e.g., due to the accumulation of iron in the plaques, which is an age-related phenomenon. Thus these protocols can only be performed in old animals (typically after 9 months (3)). Furthermore, with these methods, small plaques cannot be detected because of the low resolution of MRI. On the contrary, evaluation of T_2 relaxation times in the subiculum allows quantitation of amyloid load at very early stages of its development in a noninvasive way, and before iron has started to be detectable in the plaques by histological methods. Also, as T_2 measures reflect an "averaged" effect within each voxel, all plaques (even small ones) are expected to participate in the detected T_2 modifications. Such a "global" effect is similar to that detected in humans with other markers, such as PET agents (29). The only requirement for using T_2 measures to follow plaque deposition is to focus on brain regions with high amyloid content, such as the subiculum, where the amyloid load was above 7% even in young animals.

In conclusion, we have shown that T_2 measures allow the detection of plaques in young animals at early stages of the pathological process. This makes T_2 a potentially useful marker for evaluating the effects of drugs aimed at slowing down brain amyloidosis at a preclinical stage.

ACKNOWLEDGMENTS

We thank the Sanofi-Aventis Neurodegenerative Disease Group for the generous gift of the animals involved in this study. We are grateful to F. Francis for carefully reading and correcting the manuscript.

REFERENCES

1. Jellinger KA, Bancher C. Neuropathology of Alzheimer's disease: a critical update. J Neural Transm Suppl 1998;54:77–95.
2. Hardy J, Selkoe DJ. The amyloid hypothesis of Alzheimer's disease: progress and problems on the road to therapeutics. Science 2002;297: 353–356.
3. Jack CR, Jr., Wengenack TM, Reyes DA, Garwood M, Curran GL, Borowski BJ, Lin J, Preboske GM, Holasek SS, Adriany G, Poduslo JF. In vivo magnetic resonance microimaging of individual amyloid plaques in Alzheimer's transgenic mice. J Neurosci 2005;25:10041–10048.
4. Zaim Wadghiri Y, Sigurdsson EM, Sadowski M, Elliott JI, Li Y, Scholtzova H, Tang CY, Aguilnaldo G, Pappolla M, Duff K, Wisniewski TM, Turnbull DH. Detection of Alzheimer's amyloid in transgenic mice using magnetic resonance microimaging. Magn Reson Med 2003;50: 293–302.
5. Poduslo JF, Curran GL, Peterson JA, McCormick DJ, Fauq AH, Khan MA, Wengenack TM. Design and chemical synthesis of a magnetic resonance contrast agent with enhanced in vitro binding, high blood-brain barrier permeability, and in vivo targeting to Alzheimer's disease amyloid plaques. Biochemistry 2004;43:6064–6075.
6. Higuchi M, Iwata N, Matsuba Y, Sato K, Sasamoto K, Saido TC. (19)F and (1)H MRI detection of amyloid beta plaques in vivo. Nat Neurosci 2005;8:527–533.
7. Helpern JA, Lee SP, Falangola MF, Dyakin VV, Bogart A, Ardekani B, Duff K, Branch C, Wisniewski T, de Leon MJ, Wolf O, O'Shea J, Nixon RA. MRI assessment of neuropathology in a transgenic mouse model of Alzheimer's disease. Magn Reson Med 2004;51:794–798.
8. Falangola MF, Ardekani BA, Lee SP, Babb JS, Bogart A, Dyakin VV, Nixon R, Duff K, Helpern JA. Application of a non-linear image registration algorithm to quantitative analysis of T_2 relaxation time in transgenic mouse models of AD pathology. J Neurosci Methods 2005;144: 91–97.
9. El Tannir El Tayara N, Delatour B, Le Cudennec C, Guegan M, Volk A, Dhenain M. Age-related evolution of amyloid burden, iron load, and MR relaxation times in a transgenic mouse model of Alzheimer's disease. Neurobiol Dis 2006;22:199–208.
10. Falangola MF, Lee SP, Nixon RA, Duff K, Helpern JA. Histological co-localization of iron in Abeta plaques of PS/APP transgenic mice. Neurochem Res 2005;30:201–205.
11. Hallgren B, Sourander P. The effect of age on the non-haemin iron in the human brain. J Neurochem 1958;3:41–55.
12. Maynard CJ, Cappai R, Volitakis I, Cherny RA, White AR, Beyreuther K, Masters CL, Bush AI, Li QX. Overexpression of Alzheimer's disease amyloid-beta opposes the age-dependent elevations of brain copper and iron. J Biol Chem 2002;277:44670–44676.
13. Takahashi S, Takahashi I, Sato H, Kubota Y, Yoshida S, Muramatsu Y. Age-related changes in the concentrations of major and trace elements in the brain of rats and mice. Biol Trace Elem Res 2001;80:145–158.
14. Blanchard V, Moussaoui S, Czech C, Touchet N, Bonici B, Planche M, Canton T, Jedidi I, Gohin M, Wirths O, Bayer TA, Langui D, Duyckaerts C, Tremp G, Pradier L. Time sequence of maturation of dystrophic neurites associated with Ab deposits in APP/PS1 transgenic mice. Exp Neurol 2003;184:247–263.

15. Paxinos G, Franklin KBJ. The mouse brain in stereotaxic coordinates. San Diego: Academic Press; 2001.
16. Puchtler H, Sweat F, Levine M. On the binding of Congo red by amyloid. J Histochem Cytochem 1962;10:355–364.
17. Delatour B, Guegan M, Volk A, Dhenain M. In vivo MRI and histological evaluation of brain atrophy in APP/PS1 transgenic mice. Neurobiol Aging 2006;27:835–847.
18. Nguyen-Legros J, Bizot J, Bolesse M, Pulicani J-P. "Noir de diaminobenzidine": une nouvelle méthode histochimique de révélation du fer exogène ["Diaminobenzidine black": a new histochemical method for the visualization of exogenous iron]. Histochemistry 1980; 66:239–244.
19. Turlin B, Loreal O, Moirand R, Brissot P, Deugnier Y, Ramee MP. Détection histochimique du fer hépatique [Histochemical detection of hepatic iron. A comparative study of four stains]. Ann Pathol 1992;12: 371–373.
20. Masuda T, Kasai T, Satodate R. Quantitative measurement of hemosiderin deposition in tissue sections of the liver by image analysis. Anal Quant Cytol Histol 1993;15:379–382.
21. LeVine SM. Iron deposits in multiple sclerosis and Alzheimer's disease brains. Brain Res 1997;760:298–303.
22. Smith MA, Harris PL, Sayre LM, Perry G. Iron accumulation in Alzheimer disease is a source of redox-generated free radicals. Proc Natl Acad Sci USA 1997;94:9866–9868.
23. Perez JM, Josephson L, O'Loughlin T, Hogemann D, Weissleder R. Magnetic relaxation switches capable of sensing molecular interactions. Nat Biotechnol 2002;20:816–820.
24. Wirths O, Multhaup G, Czech C, Feldmann N, Blanchard V, Tremp G, Beyreuther K, Pradier L, Bayer TA. Intraneuronal APP/A beta trafficking and plaque formation in beta-amyloid precursor protein and presenilin-1 transgenic mice. Brain Pathol 2002;12:275–286.
25. Tseng BP, Kitazawa M, LaFerla FM. Amyloid beta-peptide: the inside story. Curr Alzheimer Res 2004;1:231–239.
26. Braakman N, Matysik J, van Duinen SG, Verbeek F, Schliebs R, de Groot HJ, Alia A. Longitudinal assessment of Alzheimer's beta-amyloid plaque development in transgenic mice monitored by in vivo magnetic resonance microimaging. J Magn Reson Imaging 2006;24:530–536.
27. Grohn OH, Kettunen MI, Penttonen M, Oja JM, van Zijl PC, Kauppinen RA. Graded reduction of cerebral blood flow in rat as detected by the nuclear magnetic resonance relaxation time T2: a theoretical and experimental approach. J Cereb Blood Flow Metab 2000;20:316–326.
28. Niwa K, Kazama K, Younkin SG, Carlson GA, Iadecola C. Alterations in cerebral blood flow and glucose utilization in mice overexpressing the amyloid precursor protein. Neurobiol Dis 2002;9:61–68.
29. Klunk WE, Engler H, Nordberg A, Wang Y, Blomqvist G, Holt DP, Bergstrom M, Savitcheva I, Huang GF, Estrada S, Ausen B, Debnath ML, Barletta J, Price JC, Sandell J, Lopresti BJ, Wall A, Koivisto P, Antoni G, Mathis CA, Langstrom B. Imaging brain amyloid in Alzheimer's disease with Pittsburgh compound-B. Ann Neurol 2004;55:306–319.